High-accuracy surface figure measurement of silicon mirrors at 80K

Peter Blake[*a], Ronald G. Mink[a], John Chambers[a], Pamela Davila[a], F. David Robinson[a,b],
[a] Goddard Space Flight Center, Code 551, Greenbelt, MD 20771
[b] Orbital Sciences Corporation, 7500 Greenway Center Drive, Suite 700, Greenbelt MD 20770

ABSTRACT

This report describes the equipment, experimental methods, and first results at a new facility for interferometric measurement of cryogenically-cooled spherical mirrors at the Goddard Space Flight Center Optics Branch. The procedure, using standard phase-shifting interferometry, has an standard combined uncertainty of 3.6 *nm* rms in its representation of the two-dimensional surface figure error at 80, and an uncertainty of ± 1 *nm* in the rms statistic itself. The first mirror tested was a concave spherical silicon foam-core mirror, with a clear aperture of 120 *mm*. The optic surface was measured at room temperature using standard "absolute" techniques; and then the change in surface figure error from room temperature to 80 K was measured. The mirror was cooled within a cryostat, and its surface figure error measured through a fused-silica window. The facility and techniques will be used to measure the surface figure error at 20K of prototype lightweight silicon carbide and Cesic™ mirrors developed by Galileo Avionica (Italy) for the European Space Agency (ESA).

1. INTRODUCTION

The Optics Branch of the Goddard Space Flight Center (GSFC), interested in staying abreast of the rich, almost explosive, development in new materials and forms for lightweight space-based astronomical mirrors, is developing its interferometry capabilities to new levels of precision. New programs such as the James Webb Space Telescope (JWST), dedicated to studies of the early universe and passively cooled to about 35 Kelvin -- a temperature required by the scientific spectral bandpass from 0.6 microns to 28 microns[1] -- present requirements for aspheric optical components with highly accurate surface figures combined with requirements for lightweightedness and retention of figure at cryogenic temperatures. These requirements have forced more careful attention to the minimization and measurement of uncertainty.

The requirements listed above have been parceled into two metrology programs. The measurement of the mirror for the proposed Solar High Angular Resolution Photometric Imager (SHARPI) program presents the problem of high precision measurement of an asphere[2]; and the GSFC SiC Precision Cryo Mirror test program presents the problem of high precision measurement at cryogenic temperatures.

This paper presents our progress to date on the high-precision cryogenic facility. The facility is baselined for spherical mirrors with a radius of curvature (ROC) of 600 *mm*, and a clear aperture of 120 -- 150 *mm*. Our near-term goal is to achieve uncertainties of 4 *nm* rms in the measurement of surface figure errors (SFE) at the temperature of 20K.

The goals of the currently-reported experiment were:

1) Obtain the best possible estimates of the test mirror surface figure error (SFE) at both ambient conditions (room temperature) and at cryogenic temperatures. By SFE, we are referring to the two-dimensional map of deviation from the best-fit sphere; and we will use the terms figure, surface figure, and surface figure error synonymously.
2) Determine the uncertainty of these measurements.

* peter.n.blake@nasa.gov; phone 301 286-4211; fax 301 286-0204

2. TEST MIRROR AND TEST CONDITIONS

The first mirror tested was a silicon foam-core mirror, concave spherical with radius of curvature of 600 *mm* and a clear aperture of 120 *mm*. The mirror was made by the Schafer Corporation in 2001, and is an early example of their SLMS™ technology[3].

The mirror is built up from a core of open-cell silicon foam, the surface of which is closed-out with polycrystalline silicon, ground and lapped to the precise shape needed, then coated with a CVD silicon coating for super-polishing.

Fig. 1. Silicon foam-core test mirror

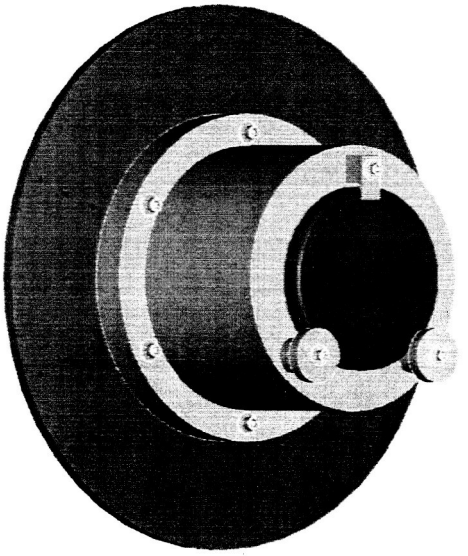

Fig. 2. Simple support on cold plate

The focus in this report is the development of procedures which deliver the highest possible accuracy and precision. It was therefore decided that there would be no sources of mechanical strain introduced into the mirror by differential thermal contractions in the mount or in the heat strapping. The mirror would be simply-supported on two support points, with its flat back resting against the cold plate (fig. 2). There would be no constraint of the mirror and no thermal straps connected to the mirror.

The cold plate and inner shroud, which surround the mirror, except for the aperture, can be lowered to 12K with liquid helium. But with no heat straps and no thermal medium joining the mirror to the cold plate – just the three points of contact – the temperature performance of the mirror was unknown. Since radiative heat transfer scales as the fourth power of absolute temperature, once the mirror temperature falls below about 100K, the cooling of the mirror was expected to be slow, and would be countered by the small amount of radiation coming from the window at room temperature. As it turns out, the mirror reached a temperature of 95K with liquid nitrogen and 80K with liquid helium.

3. FACILITY

The test facility for cryo-measurement of the prototype mirrors was described in an earlier paper by these authors[4]. A Zygo "Verifire AT"® phase measuring interferometer, positioned on crossed rails, focuses through a window into a cryostat or dewar. The cryostat has tip/tilt controls. The whole facility rests on a curtained vibration isolation table.

The cryostat is of the horizontal continuous flow type (figure 3). Cooling is provided by flowing liquid nitrogen (LN_2) or liquid helium (LHe) from storage dewars to the cold finger. The work surface is a copper plate, 15" in diameter. An

outer cylinder holds the work volume in vacuum, within which is a shuttered insulation-blanketed intermediate shroud, cooled by coupling to the exhaust gas tube by a circular flange. Within that volume is an inner shroud, bolted to the cold plate. The apertures of the vessel and the shrouds can be easily modified.

A simple redesign takes advantage of the converging interferometer beam for the testing of a 600 *mm* ROC sphere. We are able to use a small window and place it close to the focal point of the interferometer (figure 4) using a cylindrical extension that has been placed over the original window. There are several significant advantages:

a a small window can be thinner for a given deflection under vacuum, leading to less spherical aberration;

b a small footprint of the beam on the window makes it easier to achieve low transmitted wavefront error (WFE);

c placing the window 600*mm* from the mirror on a narrow extension cylinder lowers the radiative coupling between the mirror and the window, lessening the mutual distortions of the window and the mirror.

tk: new B&W photo showing transfer lines and sling

Figure 3: Dewar

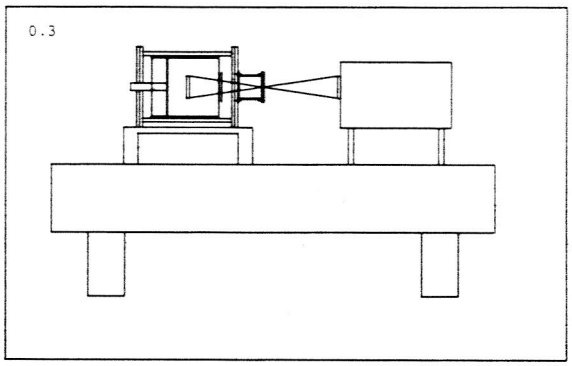

Figure 4: Dewar with window and snout added

Clear aperture diameter of test mirror (prototype)	120 *mm*
Test mirror radius of curvature (ROC)	600 *mm*
f/# of interferometer transmission sphere (TS)	3.2 nominal, 3.37 design
Design distance of cryostat window from mirror vertex	612.7 *mm*
Spot size of beam on front surface of window	4.26 *mm*
Window thickness	6.35 *mm*
Window material	fused silica: Corning 7980, class A-0

Table 1: Optical Design Parameters for the Interferometer and Cryostat

4 CORRECTION OF SYSTEMATIC EFFECTS

As will be seen in the discussion of uncertainty analysis, we confined our search for and correction of systematic effects to those whose contribution to the SFE measurement was greater than 0.5 *nm* rms.

4.1 Window Aberrations

The primary systematic effect that requires correction is the aberration of the beam as it passes twice through the window of the cryostat. This aberration has been modeled using the software program Zemax®, as described in the authors' previous paper[4]. A physical window in the cryostat was itself measured interferometrically as the cryostat was taken through the thermal cycles in a shakedown run. The Zemax® model was prepared for a Fizeau-interferometric test of a 600*mm* ROC, 150*mm* diameter spherical mirror, and contained a window identical in its parameters to the window measured in the cryostat; and the effects of the window were determined under all conditions of the upcoming thermal cycles.

It was found that if the optic axis were perpendicular to the window of the cryostat, the only aberration that contributed an SFE error of greater than 0.5 *nm* rms was spherical aberration, which contributed an error of 8.8 *nm* rms.

It was found, however, that if the window were tilted, not only were there added contributions of coma and astigmatism (ck), but the amount of aberration depended on the distance of the mirror from the window. Since we had no control over this distance or any way to measure it, it was determined to keep the angle of the optic axis to the window less than 0.4 *arcmin*, giving an error of less than 0.5 *nm* rms over and above the aberration at perpendicularity. This topic is returned to in the discussion of uncertainty analysis (section 8).

The window aberrations can be removed by two different calculations: 1) by subtracting the modeled or calculated aberrations from the final measured SFE; and 2) by measuring the change in SFE that occurs with the test mirror in the cryostat – behind the window – as the temperature drops from RT to cryogenic temperature (80K). When the measurement at room temperature and vacuum is subtracted from the measurement at 80K, the window aberrations of the two measurements -- already shown by modeling to be different by less than 0.1 *nm* rms[3], and thus negligible – are eliminated.

The method chosen should be the method with the least uncertainty. Our baseline approach is the second: finding the change upon cooling (the "cryo-deformation" or the "cryo-difference map") and adding this to the unwindowed room temp ("ambient" or "STP") surface figure error.

4.2 Interferometer Errors

The only systematic effect above 0.5 *nm* rms in the interferometer itself is imperfection of the reference surface in the transmission sphere. This error can be measured and subtracted by a technique called "absolute measurement" or the "two-sphere test"[5,6]. This technique will give a corrected map of the test mirror SFE; and recalculated, will yield a map of the interferometer errors over the pupil. This map can be used as an error file to correct the interferometer reference surface error when measuring test mirrors that do not lend themselves to the two-sphere test. For example, the ESA mirrors to be measured soon in our lab have integral feet for mounting, and would not be suitable for the two-sphere test, since gravity would force variations in surface figure as the mirror was rotated.

5 UNCERTAINTY DEFINED

5.1 Defining the Problem

Consider a result of an optical test W, which is an estimate of a surface figure. The result W is a set of N data points $\{w_1, w_2, ..., w_n,\}$ over a two-dimensional array. This measurement is the sum of the true surface figure error S, several contributions of systematic effects, and several contributions of statistical noise and unknown error[7]. We will make efforts to remove the systematic effects, as described in section 4, but each correction has itself an unknown error. The terminology becomes much clearer when we adopt the conception of *uncertainty*, as defined by NIST and ISO[7,8].

5.2 Definition of Uncertainty

We refer for our conception of uncertainty to "Guidelines for Evaluation and Expressing the Uncertainty of NIST Measurement Results", from National Institute for Standards and Technology (NIST)[8]. (These concepts are identical to those in the ISO "Guide to the Expression of Uncertainty in Measurement"[9]).

> "Basic to the [ISO] approach is representing each component of uncertainty that contributes to the uncertainty of a measurement result by an estimated standard deviation, termed standard uncertainty, with suggested symbol u_i ..."

An uncertainty component, then, can be statistically determined – the statistically estimated standard deviations s_i, and the associated number of degrees of freedom v_i; or it may be approximated: "obtained from an assumed probability distribution based on all the available information."

> "The **combined standard uncertainty** of a measurement result, suggested symbol u_c, is taken to represent the estimated standard deviation of the result. It is obtained by combining the individual standard uncertainties u_i (and covariances as appropriate)...using...the *law of propagation of uncertainty*, the "root-sum-of squares"...or "RSS" method of combining uncertainty components estimated as standard deviations....
>
> It is assumed that a correction (or correction factor) is applied to compensate for each recognized systematic effect that significantly influences the measurement result and that every effort has been made to identify such effects. The relevant uncertainty to associate with each recognized systematic effect is then the standard uncertainty of the applied correction."

Our task, then, is to estimate each individual uncertainty component, and sum them in quadrature. Since our goal is an uncertainty of about 4 *nm rms*, we limited our search to uncertainty components that were greater than 0.5 *nm rms*, since ten such uncertainties would add in quadrature to increase the total uncertainty by less than 10%.

5.3 Uncertainty as a root mean square

The root mean square (rms) of the surface deformation is a quantitative measure of the quality and performance of an optic, and, as such, is the final figure of merit in many investigations.

But how do we speak of the uncertainty of the surface figure itself – not the uncertainty of the rms figure, but the uncertainty of the two-dimensional map which is our estimate of the surface? The measurements, the corrections, and the final estimate of SFE are all maps over two dimensions. The uncertainties are not maps, *per se*, because they are unknown; but they are two-dimensional.

An approach has been suggested Ulf Griesmann, NIST[10]. The reported SFE is the sum of the true surface figure error S and unknown error. This error, although unknown, has an rms value. Our estimate of the rms value of the error is what we shall call the uncertainty of the measurement.

For example, following Griesmann, the short-term statistical component of uncertainty can be estimated by the following procedure:

a Make multiple identical measurements (e.g., twenty times).

b Average the multiple plots.

c Subtract the mean plot – pixel by pixel -- from each measurement, to form what we'll call a delta.

d Calculate the rms deviation of each of the deltas.

e Determine the distribution of the rms values of the deltas: e.g., plot a histogram of frequency vs. rms; find the mean of the distribution and the standard deviation, s.

f The uncertainty of the multiple measurements is defined such that 68% of the rms values are smaller than the uncertainty (68% confidence level analogous to the standard deviation). Thus uncertainty = mean + 0.468 * s.

Because our interest is often in the surface figure itself, or in the power spectral density, we will carry though all computations of uncertainty as computations of the uncertainty of the surface figure, not uncertainty of the rms value itself, which can be calculated at the end.

6 MEASUREMENTS

6.1 Temperature cycles

Temperatures inside the dewar and in the test mirror were measured with temperature-sensing diodes. In order to limit the thermo-mechanical strain caused by attachment of diodes to the optic, the diodes were wired with 42 gage copper and attached to the mirror edge with a thin layer of GE Varnish.

When the cold plate was held at liquid nitrogen (77K), the mirror cooled down to 95K. When the cold plate was held at liquid helium temperature, the mirror cooled only to 80K, as shown in figure 5. When the rate of change of the mirror fell below 1K/15 min., the mirror was judged to be stable enough for measurement, and the SFE was measured.

The mirror was subjected to three thermal cycles, with measurements taken at the following points:

RTP: ambient conditions, room temperature, no window, no vacuum

RTV: Measurement taken through the window. Test mirror in dewar at room temperature under vacuum.

95K: Cold plate at liquid nitrogen temperature, mirror at 95K

80K: Cold plate at liquid helium temperature, mirror at 80K

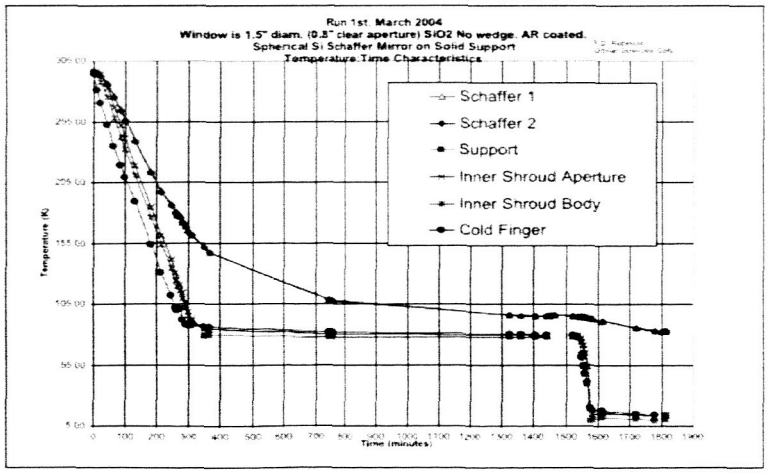

Figure 5: Temperatures during cooldown.

When the rate of cooling was 1K/hr, the shutter was opened and the radiation from the window halted the cooling. On opening the shutter, the image is nulled and the measurement taken, as the mirror rises in temperature at close to 2K/hr.

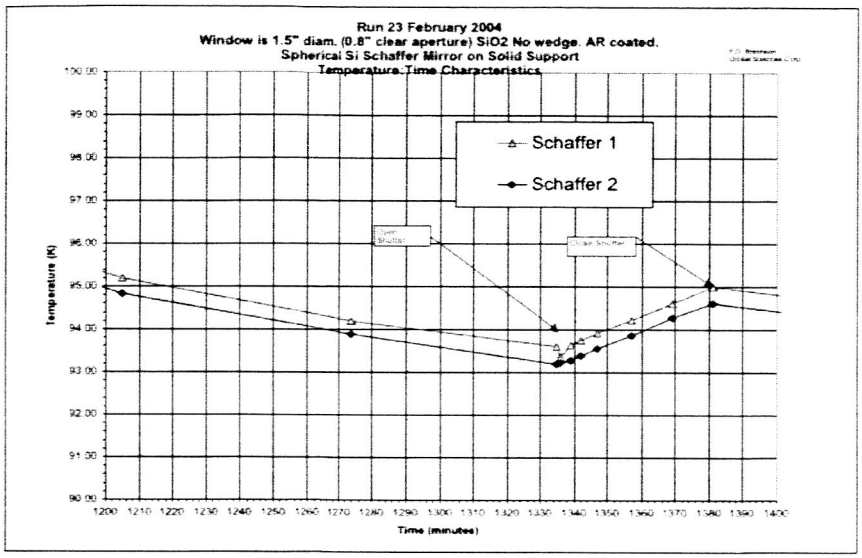

Figure 6: After 20-22 hours

6.2 Interferometer measurements

For each measurement step of the thermal cycle, twenty successive individual measurements were taken, each using thirty-two phase averages.

7 RESULTS

7.1 Two-sphere test

Early in the program, a very careful two-sphere test was performed on the test mirror. The resultant SFE was found to be 21.7 *nm* rms, or 23.2 *nm rms* at 90% clear aperture (CA).

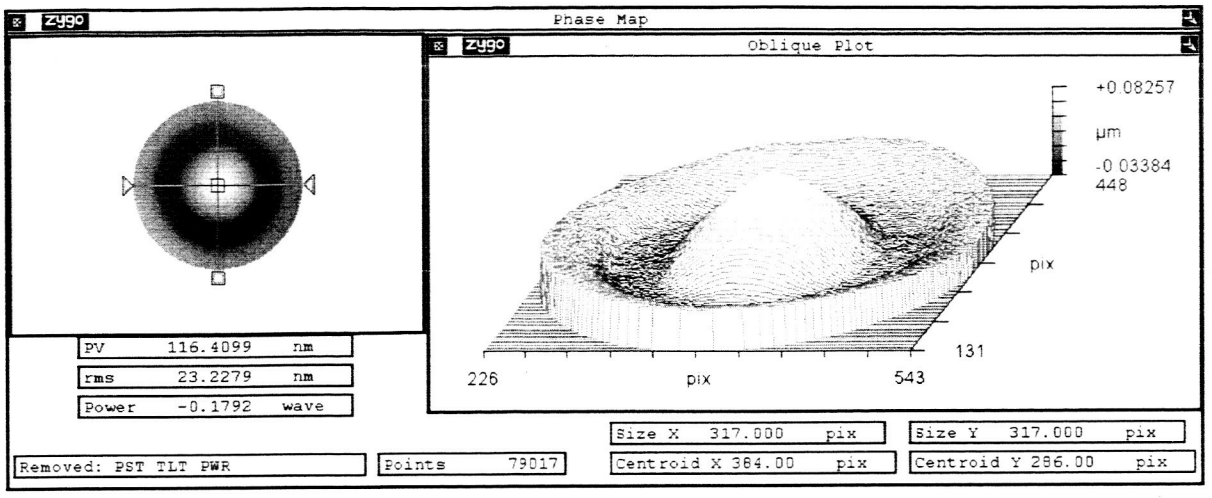

Figure 7: Two-sphere test of Schafer mirror

When this test was performed, we overlooked the utility of placing fiducials on the test mirror. So even though we have a highly accurate two-sphere test of this mirror, we could not use that measurement as our RTP measurement -- the basis for determining the surface figure at 80K. Nevertheless, this two-sphere test also gave us a map of the error of a portion of the transmission sphere, which we compared to the matching portion of the error file supplied by the Zygo corporation, and found them to agree within 1.4 *nm rms.*

Therefore, in the cryo-cycling trials reported here, our correction for the error of the reference surface was to subtract the matching portion of the Zygo error file.

7.2 Change on cooling

Both systematic errors – window aberration and reference surface error -- are subtracted out when the data file for the mirror in the dewar, in vacuum at room temperature (RTVac or RTV) is subtracted from the data file for the mirror at 80K. This subtraction was made, after registering the files as closely as possible, and the result was a cryo-change difference map with an rms of 4.9 *nm rms.*

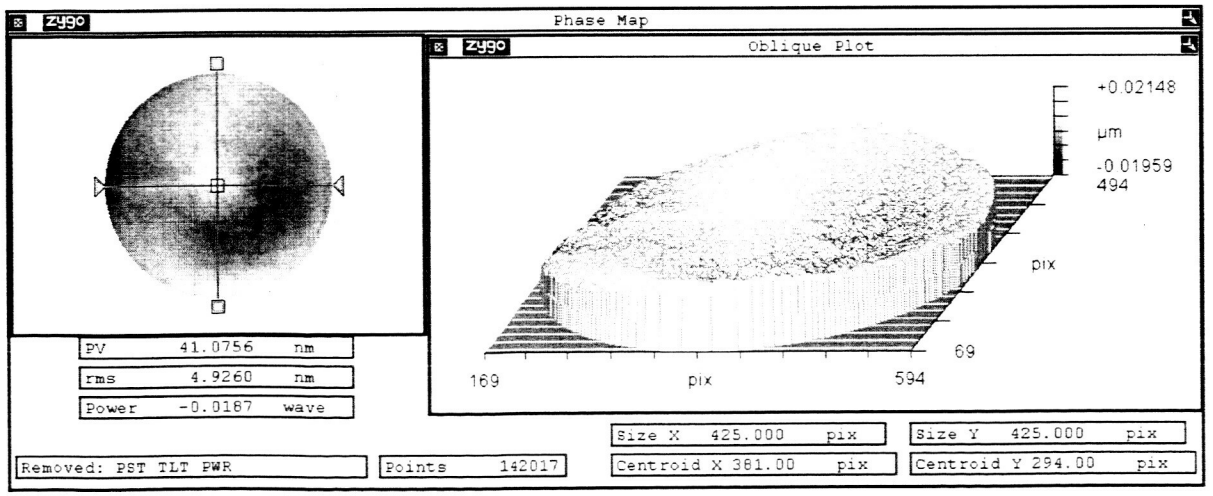

Figure 8: Change of Schafer mirror from room temperature to 80K

7.2 Surface figure at 80K

When the cryo-change difference map is added to the ambient condition measurement (corrected for reference surface error) the resultant SFE, 90% CA, has an RMS of 24.9 *nm*.

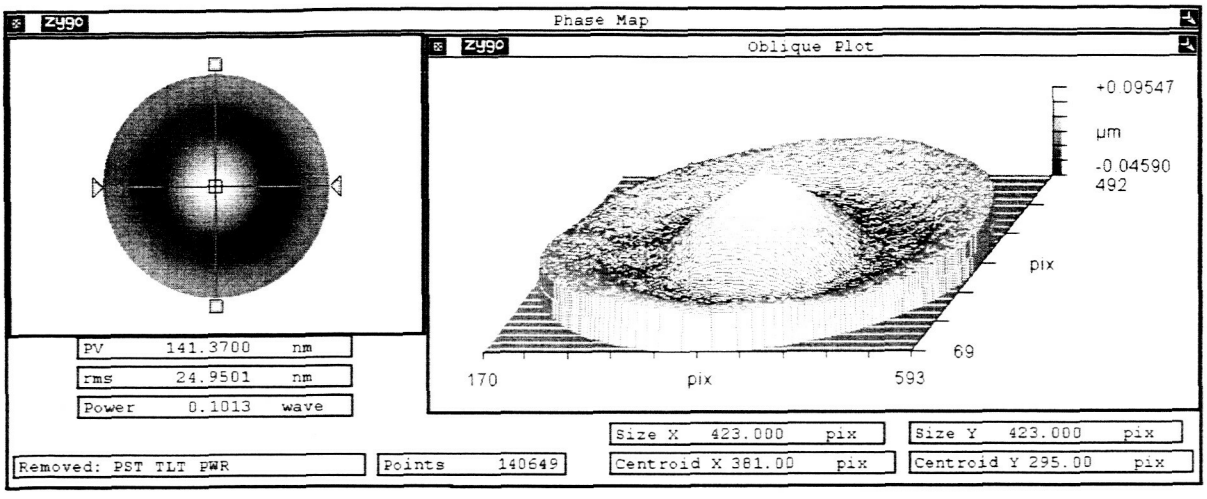

Figure 9: Surface figure error at 80K

8 UNCERTAINTY ANALYSIS

8.1 Short-term statistical Uncertainty

When the twenty individual measurements are averaged, and the deviation of each measurement is subtracted from the mean, the short-term variation can be measured.

The results:

- -- at RTP, the short-term statistical uncertainty is: 0.7 *nm* rms
- -- at RTV, the short-term statistical uncertainty is: 0.9 *nm* rms
- -- at 95K, the short-term statistical uncertainty is: 0.8 *nm* rms
- -- at 80K, the short-term statistical uncertainty is: 1.2 *nm* rms

This is the uncertainty of any of the individual measurements. The mean of all twenty measurements for a condition would have lower uncertainty. The numbers quoted above include some OPD arithmetic uncertainty (see below); so an estimated short-term uncertainty of $\frac{1.2nm}{\sqrt{20}}$ turns out to be a reasonable estimate of the short-term statistical contribution.

8.2 Long-term statistical Uncertainty

A measure of the long-term statistical uncertainty was made in a previous experiment[4], and was found to contribute (in RSS) an additional 0.8 *nm rms* to the statistical uncertainty.

8.3 OPD arithmetic Uncertainty

Another error enters in when the data sets, maps of the SFE measured over the pixel plane, are aligned, scaled to congruence, and added or subtracted: a process we call OPD (optical path difference) arithmetic. For each individual addition or subtraction of wavefronts, a good estimate can be made of the uncertainty of position of the sets – the uncertainty of registration and congruence, pixel-for-pixel. The resultant error in the SFE stemming from that degree of misregistration can be quickly determined by taking an individual measurement, translating or mis-aligning it by that degree and subtracting it from the original. This estimation was done for every such addition or subtraction of data sets, with the calculated uncertainties ranging between 0.5 *nm* rms and 1.7 *nm* rms.

8.4 Optic Axis Alignment Uncertainty

Our technique for aligning the optic axis to the dewar window[11] was accurate to within one pixel of the camera, which translates to an uncertainty of 0.4 *nm* rms.

8.5 Uncertainty of error file

As discussed in section 7.1, we utilized the error file produced for us by the Zygo corporation. They used a two-sphere test of the transmission sphere in our interferometer to produce the error file, which had an RMS of 4.4 *nm*. We found it best to characterize this transmission sphere error by the first 36 Zernikes of the measured error file. Using only the first 36 zernikes entails dispensing with the residual, and adds an additional uncertainty of 1.3 *nm*.

In addition to this, there is an uncertainty in the error file itself. This was not determined by Zygo. So we estimate the uncertainty by examining the difference between two independent measurements: Zygo's measurement (using a convex mirror in a short cavity) and our own two-sphere measure of the transmission sphere, using the test mirror in the same cavity as is used in measuring the test mirror. This measurement suffers the sole flaw of not filling the pupil, *ie*, not measuring the whole reference surface, but just a portion of it. Over that portion, the two measurements differed by 1.4 *nm rms*; and that figure was taken as a conservative estimate of the uncertainty of the reference surface.

When, in 7.2, the two measurement files for 80K and RTV are subtracted, the error due to the transmission sphere reference surface is subtracted out of the final result – if the two files occupy the same space in the pupil. If not, there is small error contributed by the shear of the error file. This error is smaller than the OPD arithmetic necessary to eliminate it, so the uncertainty of the OPD arithmetic was conservatively assigned to this factor.

8.6 Combined Standard uncertainty

Combining these uncertainties in standard RSS form, with individual contributions from each iteration of OPD arithmetic, gives us an uncertainty in our map of cryo-deformation of 2.2 *nm rms*.

In a rough estimate, the true rms of the cryo-deformation would range between the RSS sum and difference of the determined cryo-deformation of 4.9 *nm rms* and the determined uncertainty of 2.2 *nm rms*, *i.e.*, between 4.4 *nm* and 5.4 *nm rms*. Thus, our estimate of the cryo-deformation is determined to be 4.9 ± 0.5 *nm rms*.

The cryo-deformation is not independent of the ambient condition SFE, so the expected surface figure is better obtained by adding the cryo-change to the ambient SFE, and taking the rms of the result.

8.7 Predicted Combined Standard uncertainty for the Galileo Avionica mirrors

The mirrors produced by Galileo Avionica for ESA's technology demonstration program have been received by our laboratory and will be measured over the coming weeks, utilizing the same methods and the same uncertainty analysis. The value for the uncertainty will change; but the values obtained in the experiment reported in this paper can be taken as conservative estimates.

9 CONCLUSION

Procedures have been developed to measure the silicon carbide and silicon carbide composite mirrors made for ESA by Galileo Avionica as technology demonstrators for the NIRSpec program, and to determine the SFE of these mirrors at 20K, with an estimated uncertainty in the OPD map of about 3.6 *nm rms,* and an uncertainty in the rms figure itself of ± 1 *nm rms.*

ACKNOWLEDGEMENTS

The authors gratefully acknowledge the assistance of the Schafer Corporation, the European Space Agency, and the James Webb Space Telescope. Our thanks also to Chip Frohlich and Badri Shirgur of the Swales Corporation, Beltsville MD, and to Joe McMann of Mantech Systems Engineering Corp., Greenbelt, for their expert assistance on many aspects of this program. Special Thanks also to Ulf Griesmann, NIST.

Mention of trade names or commercial products does not constitute endorsement or recommendation by NASA.

REFERENCES

[1] B. D. Seery, "The James Webb Space Telescope (JWST): Hubble's Scientific and Technological Successor," *Proc SPIE*, **4850** pp170-178, 2003.

[2] S. Antonille, "High Precision Figure Verification of a Lightweight UV Mirror," internal report, Goddard Space Flight Center, Optics Branch, Greenbelt MD, 2003

[3] Marc T. Jacoby, *et. al.*, "Helium cryo-testing of a SLMS™ (silicon lightweight mirrors) athermal optical assembly, *Proc SPIE 5180, Optical Manufacturing and Testing V,* ed. Phil Stahl, pp199-210, 2003

[4] P. Blake, R. G. Mink, D. Content, P. Davila, F. D. Robinson, S. R. Antonille, "Techniques and uncertainty analysis for interferometric surface figure error measurement of spherical mirrors at 20K", *Proc SPIE, 5180, Optical Manufacturing and Testing V,* ed. Phil Stahl, pp188-198, 2003.

[5] J. E. Greivenkamp, J.H. Bruning, "Phase Shifting Interferometers", in *Optical Shop Testing, 2nd ed.*, D. Malacara, ed., pp577-580, John Wiley & Sons, NY, 1992

[6] K. Elssner, R. Burow, J. Grzanna, R.Spolaczyk, "Absolute Sphericity Measurement," *Applied Optics,* **28**, pp 4649-4661, 1989

[7] A. Davies, M.S. Levenson, "Estimating the root mean square of a wave front and its uncertainty", *Applied Optics*, **40**, pp 6203-6209, 2001

[8] B. Taylor, C.E. Kuyatt, "Guidelines for Evaluation and Expressing the Uncertainty of NIST Measurment Results", NIST Technical Note 1297, 1994

[9] ISO, *Guide to the Expression Uncertainty in Measurement,* International Organization for Standardization, Geneva, Switzerland, 1993.

[10] Ulf Griesmann, National Institute of Standards and Technology, Gaithersburg, MD, personal communication.

[11] To be published in *NASA Tech Briefs*